1684 *Macromolecules* **2007,** *40,* 1684−1692

Brownian Molecular Dynamics Simulation on Self-Assembly Behavior of Rod−Coil Diblock Copolymers

Shaoliang Lin,*,[†] Naoko Numasawa,[‡] Takuhei Nose,[§] and Jiaping Lin[†]

Key Laboratory for Ultrafine Materials of Ministry of Education, School of Materials Science and Engineering, East China University of Science and Technology, Shanghai 200237, China; School of Dentistry, Nihon University, Tokyo 101-8310, Japan; and Department of Nanochemistry, Tokyo Polytechnic University, Atsugi, Kanagawa 243-0297, Japan

Received September 6, 2006; Revised Manuscript Received December 20, 2006

ABSTRACT: Brownian molecular dynamics simulations are carried out on the self-assembly behavior of rod−coil diblock copolymers. The copolymer molecule is represented by a linear chain consisting of definite beads connecting by harmonic bond stretching potential. The rigidity of the rod block is introduced by harmonic potential for bend at a substantially zero bond angle. The micelle structures formed by such copolymers and molecular packing of rod blocks are investigated. Transitions of aggregate structure are found with changing Lennard-Jones (LJ) interaction ϵ_{RR} of rod pairs. The rod blocks tend to align orientationally and pack hexagonally in the core to form a smectic-like disk structure at the higher ϵ_{RR}. With decreasing ϵ_{RR}, a disk micelle is gradually changed to a new string structure, where the twisting of rod blocks packing in the core has been discovered and further breaks into some small aggregates until unimers. The radius of gyration and order parameter of rod blocks are calculated to confirm such a transition from disk to string structure. The regions of thermodynamic stability of disk, string, and small aggregates are constructed in the diagrams of block chain length against ϵ_{RR} and temperature vs ϵ_{RR}. Increase of the rod block length leads to a more dramatic decrease of the critical micelle interaction (CMI) than decrease of the coil block length does. The onsets of string and disk formation move to higher ϵ_{RR} with decreasing rod block length and/or increasing coil length. Meanwhile, the regions of string micelle and small aggregates become wider. Some simulation results are in agreement with existing experimental observations and theoretical predictions.

Introduction

The phase behavior and morphology of block copolymers consisting of rod and coil blocks in solution as well as in melt have received much attention in both experimental[1−11] and theoretical viewpoints.[12−19] The difference in chain rigidity between rod and coil blocks is expected to greatly affect the details of molecular packing and thus the nature of thermodynamically stable supramolecular structures. Jenekhe et al. have studied the self-assembled aggregates of poly(phenylquinoline)-*b*-polystyrene rod−coil block copolymers in solution.[1,2] The morphologies of hollow spherical, vesicular, cylindrical, and lamellar aggregates have been observed by changing the solvent composition. Kallitsis et al. have reported that poly(2-hydroxyethyl methacrylate)-*b*-polystyrene rod−coil copolymers can form island, stringlike, and homeycomblike structures by increasing the selective solvent concentration in mixture solvents.[5] Stupp et al. have reported on rod−coil copolymers consisting of an elongated mesogenic rod and a monodisperse polyisoprene coil.[6,7] They found the morphology varies from alternating strips of rod- and coil-rich domains to discrete aggregates of rods arranged in a hexagonal superlattice as rod volume fraction is decreased.

For the theoretical treatment, Halperin has used scaling approaches to study the aggregation behavior of rod−coil block copolymers in a selective solvent and found a smectic A−smectic C transition within the core of micelle by comparing interfacial and coil deformation free energy.[12] Williams and Fredrickson have proposed the hockey puck micelle where the rods are packed axially into cylinders covered by coils. They predicted that the hockey puck structure should be stable at large coil fractions.[15] All of these rod−coil molecular architectures impart the rod blocks into ordered structures due to the large difference in stiffness between rod and coil blocks.

Recently computer simulation has played an important role in investigating material properties and its physics. As the computer simulation is based on a well-defined model, it can solve the unavoidable problems arising from experiments, such as molecular weight distribution and molecular composition heterogeneity. Moreover, it proceeds straightforwardly without assumptions of micelle structure and chain conformation in theoretical works.[20] Many simulation studies on the self-assembly behavior of block copolymers only consisting of flexible coil chains have been performed using various computational techniques such as Monte Carlo (MC),[21−25] molecular dynamics (MD),[26−31] and dissipative particle dynamics (DPD) simulations.[32−34] Few works have been reported on computer simulations for rod−coil copolymers.[35−39] AlSunaidi et al. used mesoscale DPD simulations to study the liquid-crystalline ordering in rod−coil diblock copolymers.[35] The isotropic, smectic A, and crystalline phases of the rodlike blocks are observed.[37] Allen et al. studied a model of hard spherocylinders attached to a flexible tail by MC simulation. They observed smectic A and crystal phases, in addition to the isotropic phase. Similar observation of stabilization of the smectic phase has been reported by McBride et al.[39] All of these literatures are focused on the liquid-crystalline behavior of rod−coil system in bulk. However, no work has been reported on computer simulation of micellization behavior of rod−coil copolymer so far, to our knowledge. It is interesting to investigate the self-

---

* To whom correspondence should be addressed: e-mail linshaoliang@hotmail.com; Tel +86-21-6425-1011; Fax +86-21-6425-3539.

[†] East China University of Science and Technology.

[‡] Nihon University.

[§] Tokyo Polytechnic University.

10.1021/ma062064l CCC: $37.00

Table 1. Conversion of the Reduced Unit System[a]

reduced unit	value
reduced length	$1\sigma = 0.4$ nm
reduced energy	$1\epsilon = 0.5$ kJ/mol
reduced mass	$1m = 23.3 \times 10^{-27}$ kg
reduced temperature	$1T = \epsilon/R = 60.1$ K
reduced time	$1t = \sqrt{A_v m\sigma^2/\epsilon} = 2.12$ ps
reduced density	$1\rho = m/\sigma^3 = 0.363$ g/cm^3
reduced pressure	$1P = \epsilon/(A_v\sigma^3) = 13.0$ MPa

[a] R is the gas constant, and A_v is Avogadro's number.

assembly behavior by focusing our attention on the different rigidity between rod and coil block and mesogenic property of rod block compared with coil−coil copolymers.

In this paper, we perform molecular dynamic simulations, using a Brownian dynamics, on the self-assembly behavior of amphiphilic rod−coil diblock copolymers to investigate micelle structure and molecular packing. The MD simulation has widely been utilized because of the advantage that comparisons with theories and experiments are straightforward. Brownian dynamics simulation has been proven to be quite efficient to study amphiphilic self-assembly.[40] The copolymer is here represented by a linear chain consisting of definite beads connecting by bond stretching potential. The rigidity of a rod block is introduced by the angle bend potential. Structural transitions of aggregates are found as change Lennard-Jones interaction of rod pairs. Diagrams for the regions of thermodynamic stability of disk, string, and some intermediate aggregates are constructed. The molecular packing and molecular order of the rod blocks in aggregates are investigated. The influences of chain length and temperature on the self-assembly behavior are also presented. Some simulation results are compared with existing experimental observations and theoretical predictions.

Method of Simulation

The simulations are performed by using the simulator, coarse-grained molecular dynamics program (COGNAC) of OCTA. The simulator was developed by Doi's group, which is public on a Web site.[41] COGNAC uses the reduced unit system for setting data. To convent it to the real unit, a set of unit parameters are given in Table 1.

Molecular Model and Simulation Conditions. To construct rod−coil diblock copolymer molecules and their assembly, potentials that should be given are bonding potential, U_{mol}, and nonbonding potential, U_{ij}. That is, the potentials that act on the beads (atoms) are divided into two parts. The former can construct a desired molecule from atoms, while the latter describes intermolecular interactions.

The rod−coil diblock copolymer molecule is represented by a linear chain consisting of several beads connecting by bond stretching potential. Hereafter, we will denote a rod−coil diblock copolymer with m rod beads and n coil beads as R_mC_n. The illustration of a rod−coil diblock copolymer molecule (for instance, R_6C_9) model is shown in Figure 1. The beads colored by blue and green are hydrophobic rod block and hydrophilic coil block, respectively. To realize the rod block R_m, angle bending potentials are combined to keep the rigidity of the molecule. Without angle bending potential constraint, the coil block is represented by a flexible chain as shown in Figure 1. Therefore, U_{mol} is a combination of $U_{\mathrm{bond}}(r)$ and $U_{\mathrm{angle}}(\theta)$. The bond stretching potential is a function of distance between the chemically bonded beads r. A harmonic type is applied and defined by

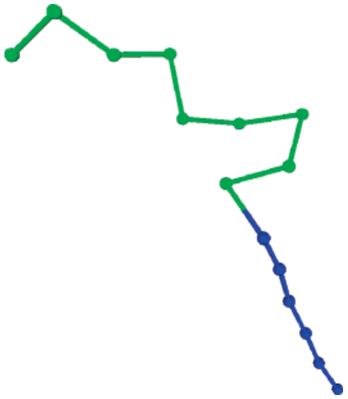

Figure 1. Layout of R_6C_9 diblock copolymer.

$$U_{\mathrm{bond}}(r) = \frac{1}{2}k_{\mathrm{b}}(r - r_0)^2 \tag{1}$$

where k_{b} is the bond spring constant and r_0 is the equilibrium bond length. The value of k_{b} is set to be 10 000, which is large enough to avoid the overstretching of bonds, for both rod and coil blocks. $U_{\mathrm{bond}}(r)$ consists of the potentials of rod block, coil block, and the junction bond of these two blocks. Setting values of bond length r_0 are 0.75, 1.0, and 1.0 for them, respectively.

For the rod block, the angle bending potential, $U_{\mathrm{angle}}(\theta)$, is a cosine harmonic function of the angle θ defined by the three chemically connected beads.

$$U_{\mathrm{angle}}(\theta) = \frac{1}{2}k_{\mathrm{a}}(\cos\theta - \cos\theta_0)^2 \tag{2}$$

where k_{a} is the angle spring constant and θ_0 is the equilibrium angle. The larger the k_{a} value, the more rigidity of the molecule chain. To realize the rod block, the equilibrium angle θ_0 is set as a value of 0.1° (substantially zero). The constant k_{a} is set to be 10 000. The realization of rod chain is the same as employed in our previous model for lyotropic liquid crystal solution.[42]

The interaction energy U_{ij} is given by the standard Lennard-Jones 12:6 potential U_{ij} acting between any pair of beads i and j:

$$U_{if} = \begin{cases} 4\epsilon_{ij}\left[\left(\dfrac{\sigma_{ij}}{r_{ij}}\right)^{12} - \left(\dfrac{\sigma_{ij}}{r_{ij}}\right)^{6} - \left(\dfrac{\sigma_{ij}}{r^{c}_{ij}}\right)^{12} + \left(\dfrac{\sigma_{ij}}{r^{c}_{ij}}\right)^{6}\right], & r \le r^{\mathrm{c}}_{\mathrm{ij}} \\ 0, & r > r^{\mathrm{c}}_{\mathrm{ij}} \end{cases} \tag{3}$$

where r^{c}_{ij} is the cutoff distance and $r_{ij} = |\vec{r}_i - \vec{r}_j|$, with $\vec{r}_i$ and $\vec{r}_j$ being the locations of the ith and jth beads, respectively. The amphiphilicity in this model is realized using a method mentioned by Bhattacharya et al.[43,44] It is introduced by a repulsive cutoff distance for the coil−coil and rod−coil ($r^{\mathrm{c}}_{\mathrm{CC}} = 2^{1/6}$, $r^{\mathrm{c}}_{\mathrm{RC}} = 2^{1/6}$) and an attractive cutoff for the rod−rod interaction ($r^{\mathrm{c}}_{\mathrm{RR}} = 2.5$). Such selections of r^{c}_{ij} make the rod block form the core of micelles. The diameter σ of LJ bead is kept to be unity for any pairs of species. The pairwise interaction ϵ_{RR} between rod and rod beads is chosen to be variable, while the other interactions are all set to be unity, i.e., $\epsilon_{\mathrm{RC}} = \epsilon_{\mathrm{CC}} = 1.0$. This set with a different value of ϵ_{RR} results in a different attractive interaction between rod beads. The choices of the LJ parameters are summarized in Table 2. As is well-known, change of the interaction between rod pairs plays an important role in the phase behavior of the LC system.[45−47] In this work, the changes of ϵ_{RR} are carried out to see influences on the micelle structures formed by rod−coil copolymers.

Table 2. Interaction Parameters for LJ Potentials

interaction	σ_{ij}	ϵ_{ij}	$r_{ij}{}^{c}$
rod−rod	1.0	1.3−3.4	2.5
rod−coil	1.0	1.0	$2^{1/6}$
coil−coil	1.0	1.0	$2^{1/6}$

All the simulations are carried out on a cubic cell (60 × 60 × 60) using a dynamic algorithm with the temperature controlling method (NVT ensemble). Brownian dynamics is applied in this work, which is developed by Grest and Kremer.[48] To simulate a constant temperature ensemble, the beads are coupled to a heat bath and the equations of motion written by

$$m_i \frac{d^2 \vec{r}_i}{dt^2} = \vec{F}_i - \Gamma \frac{d\vec{r}_i}{dt} + \vec{W}_i(t) \tag{4}$$

where m_i is the mass of the ith bead. $\vec{F}_i$ is force acting on the ith bead, which is calculated by the potential energies consisting of U_{mol} and U_{ij} related to the location of the ith bead. Γ is friction constant. In the Langevin dynamics, the effect of solvent molecules is implicitly treated by the noise term $\vec{W}_i(t)$, which can be calculated using the fluctuation−dissipation relation:[43,49]

$$\langle \vec{W}_i(t) \cdot \vec{W}_j(t') \rangle = 6k_B T \Gamma \delta_{ij}(t - t') \tag{5}$$

Periodic boundary conditions were imposed to minimize the effect of finite system size. A regular body-centered-cubic (bcc) packing lamellar mode for 100 rod−coil copolymers is applied to generate the initial structures of molecules, and the structure relaxation is done by stochastic dynamic simulation. The integration time step $\Delta t = 0.008$ was selected. The length of simulation runs was 3×10^6 time steps, i.e., 24 000 time units. All calculations were performed at a temperature $T = 3.0$ without further specification.

Order Parameter. A quantitative measure for the degree of alignment of rod blocks is the order parameter S. The order parameter S_i for the rod block coded as i can be defined by

$$S_{\mathrm{i}} = \frac{3(u_i \cdot u_d)^2 - 1}{2} \tag{6}$$

where u_i is normalized vector of the ith rod block and u_d is the normalized vector of orientation direction, which is determined by iteration to find the maximum value of S by taking into account the up−down symmetry of the rod block. The order parameter S of rod blocks within the core is calculated to be the average value of S_i.

Twisting in Rod Alignments. Here we present a mathematical method to describe a rod blocks alignment in a string micelle, where a twisting (helical-like) structure is found in the core. The rod alignment is characterized by the vector product, $u_i \cdot u_d$, of normalized vector of the ith rod block, u_i, and normalized vector of orientation direction, u_d. The product represents the angle, ψ_i, between the ith rod and orientation direction of rod blocks, expressed as

$$\cos(\psi_i) = u_i \cdot u_d \tag{7}$$

The twisting of rod blocks alignment in the core can be described by as a function of position of the rod block along the long-center axis of the string micelle. For a rigid string, the long-center axis can be illustrated by the longest distance between the rod block pairs. The pitch of twisting string can be calculated from the plot of cos(ψ) vs position along the axis. For a slightly flexible string, the long-center axis of the string should be divided into 2 or 3 subaxes. Following the calculation method mentioned above, we can calculate the pitch of the twisting string.

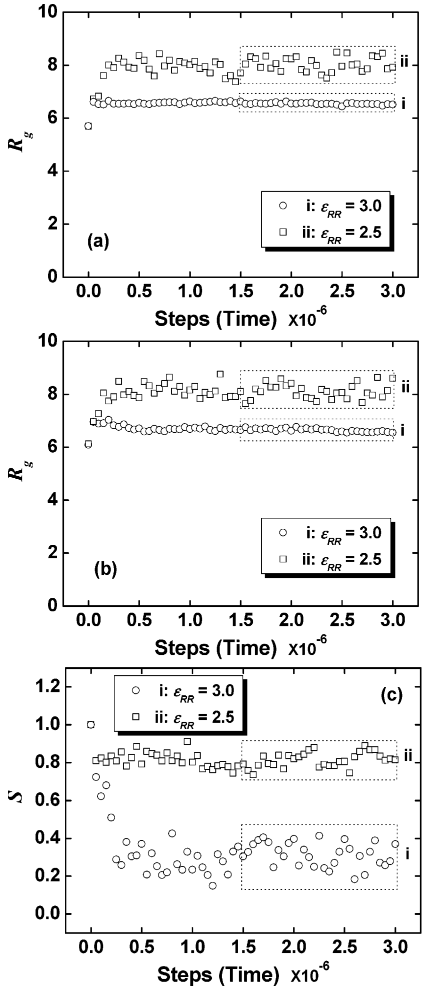

Figure 2. Time evolutions of the radius of gyration R_g for R_6C_9 copolymers from different initial structures: (a) regular square; (b) regular elongated square. (c) Time evolutions of order parameter S of rod blocks.

Radius of Gyration. To monitor the change of micelle size, we calculate the radius of gyration defined by

$$R_g = \sqrt{\frac{1}{N}\sum_{i=1}^{N}(r_i - r_c)^2} \tag{8}$$

where r_i and r_c denote the location of each bead in rod−coil chains and the center-of-mass for the whole chains, respectively. N is the total number of beads in the system.

Results

Time Evolution of Micellar Structure and Equilibrium Conditions. Before we present the simulation results, it is worthwhile to discuss the details of obtaining reliable data from the simulation. In order to analyze the micelle structure and molecular packing, the equilibrium state of micelle should be reached in a finite simulation time. Figure 2a shows two typical results of R_g of micelle as a function of simulation time for the different segregation strength ϵ_{RR} of rod pairs, where the initial structure is a regular square. The two cases are presented for the ϵ_{RR} values of 3.0 (plot i) and 2.5 (plot ii). As it can be seen, from plot i, the R_g value increases to a higher value within a short simulation time and then tends to level off, suggesting the system reaches an equilibrium condition during the simulation process. At the lower ϵ_{RR} shown as plot ii, the R_g value increases to a high value and then continually fluctuates at a low level. Such a fluctuation also indicates the system is at equilibrium. In the present calculations, 3×10^6 simulation steps are performed. All quantities of R_g are averaged over the last 1.5×10^6 steps. For example, the R_g values as calculated results for plot i and plot ii shown in Figure 2a are 6.56 and 8.03, respectively.

Initial-structure dependencies are examined to check the process dependence of obtained structure, i.e., to confirm the equilibrium. Shown in Figure 2b are simulation results of R_g when the initial structure is a regular elongated square. Time evolutions of R_g for the same values of ϵ_{RR} as used in Figure 2a are also calculated to be shown in Figure 2b. We can see that the two systems reach stationary states within 3×10^6 simulation steps. The R_g values are 6.64 and 8.07 for plot i and plot ii, respectively, which are almost same as those obtained from Figure 2a for the initial regular square structure. That is, no initial-structure dependence on the R_g values is detected, which indicates the obtained structures formed by rod−coil diblock copolymers are substantially in the equilibrium condition.

Shown in Figure 2c are time evolutions of order parameter S of rod blocks at $\epsilon_{RR} = 3.0$ (plot i) and 2.5 (plot ii). Both S values decrease from 1.0 for the regular initial structure and then tend to continually fluctuate at a low level during the simulation process. Such a fluctuation also indicates the system is substantially in equilibrium condition. We can see that the initial large changes in R_g and S before reaching stationary states are finished within a short time, about 0.3×10^6 simulation steps, in any case. Therefore, we may say that the system substantially reaches the equilibrium structure rather fast in the present time scale of simulations.

Evolution of Micelle Structure with Changing Segregation Strength of Rod Blocks. To visualize changes in micelle structure and molecular packing with changing the segregation strength ϵ_{RR} of rod blocks, typical snapshots of R_6C_9 copolymer systems are shown in Figure 3, where the rod and coil blocks are colored by blue and green, respectively. In the case of the stronger segregation of $\epsilon_{RR} = 3.1$ (snapshot i in Figure 3a), the aggregated rod blocks tend to align orientationally in the core of micelle. The snapshot ii in Figure 3a shows that the geometric structure of this micelle core is of circlelike form viewing from the vertical direction to the rod alignment axis. Here, such a micelle structure is called as a disk structure, which can be found as $\epsilon_{RR} \geq 2.9$.

At the intermediate segregation strength $2.5 \leq \epsilon_{RR} < 2.9$, a string (cylinder-like) micelle is observed. The typical snapshot for $\epsilon_{RR} = 2.6$ is shown in Figure 3b. The snapshot i illustrates an unusual molecule packing of rod block. In each section of the string micelle, the rod block tends to align in an orientation vector, and such a vector is gradually changed along the long-center axis of the string. That is, the micelle is a *twisted* string. It is notable that micelle structure is gradually changed from disk structure to string with decreasing ϵ_{RR}. Under certain ϵ_{RR} value, an ellipsoid-like structure of micelle is also found. For simplification, such a structure is regarded as a string micelle.

With further decreasing the segregation strength, the twisting string micelle is broken into small aggregates coexisting with some single copolymers (unimers), as is clearly seen from the snapshot of $\epsilon_{RR} = 2.2$ in Figure 3c. Here we call such broken micelle small aggregates. With further decreasing ϵ_{RR}, more and more unimers come out of the small aggregates. As the ϵ_{RR} is lower than a certain value (critical micelle interaction, CMI), no aggregates are formed here as $\epsilon_{RR} < 2.1$ and only free unimers distributed randomly in the system (snapshot is not included).

In summarizing the findings from the snapshot pictures shown in Figure 3, the structure transitions from disk to string and further to some broken small aggregates until free unimers occur with decreasing segregation strength ϵ_{RR} of rod pairs. The structural transitions of micelle and molecule packing of rod blocks can be identified in terms of micelle size and order parameter S. Figure 4 shows the radius of gyration R_g for R_6C_9 micelle as a function of ϵ_{RR}. R_g is stable as ϵ_{RR} is in the range 3.1−2.9 and then increases gradually with decreasing ϵ_{RR}. Such a change of R_g suggests that the structure of micelle is gradually changed with decreasing ϵ_{RR}. The R_g is not presented here for $\epsilon_{RR} < 2.5$ due to the fact that the micelle is broken in the small aggregates region. The order parameter S of rod blocks in the core vs ϵ_{RR} is presented in Figure 5. S is about 0.8 in the disk region as $\epsilon_{RR} \geq 2.9$ and then gradually decreased to about 0.3 with decreasing ϵ_{RR}. The higher S value shows that the rod blocks are orientated and packed regularly in core. The value of S deviates from 1.0 because some rod blocks are tilted at the edge of the disk structure. In the string region, the rod blocks are twistablely packing in the core of micelle, so S is decreased dramatically as shown in Figure 5, where ϵ_{RR} is between 2.5 and 2.8.

As seen in Figures 4 and 5, changes in R_g and S with change in interaction ϵ_{RR} are gradual, and no detectable indication of their large fluctuations are observed during the transition, so that the transition in micellar shape may not be a thermodynamically sharp transition, but rather a gradual change. We can here note some kinetic and dynamical aspects on the transition in micellar shape. The growths of length (elongating) and twisting take place simultaneously, which can be seen in simultaneous changes in R_g and S since the increase in R_g and the decrease in S mainly reflect the elongation and the twisting, respectively. Also, we watched the translational motion of each molecule within a micelle during the process from the regular initial structure to the disk or stringlike micelle and observe that the molecules move more frequently (quickly) on the surface than the inside. Therefore, we can speculate that, by similar diffusive motions, the aggregate shape may change from circle to elongated one, i.e., from disk to string.

To see the details of packing manner of the rod blocks in core of disk micelle, the typical distance distribution between center positions of rod blocks at $\epsilon_{RR} = 3.1$ is plotted in Figure 6a. Several peaks are exhibited, which have the peak position ratio, about $1:\sqrt{3}:2:\sqrt{7}$, suggesting rod blocks are hexagonally packing in the core of disk micelle. Shown in Figure 6b are the center positions of rod blocks for a snapshot, which are presented in the rectangular coordinates where the z-coordination axis is taken to be normal to the plane of micellar disk, to illustrate the fluctuation of the rod blocks in the orientation direction. The plane of micellar disk was determined by the least-squares fitting to center positions of the rod blocks. The rod positions are fluctuating with time in a range similar to that of this snapshot. In order to see the fluctuation of center positions of rod blocks, x- and z-component values of positions are plotted in Figure 6c, which is similar to the plot of y- and z-component values. The structure is not so fluctuating (including bending). Considering such a small fluctuation as well as the hexagonal packing (Figure 6a) with a reasonably high order parameter in

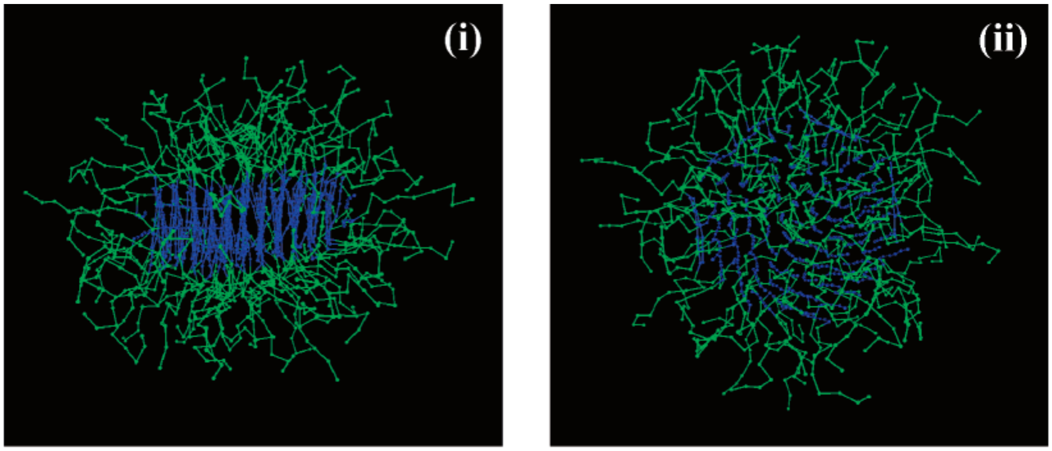

(a) $\varepsilon_{RR} = 3.1$ (i: side view perpendicular to the rod axis; ii: top view along the rod axis)

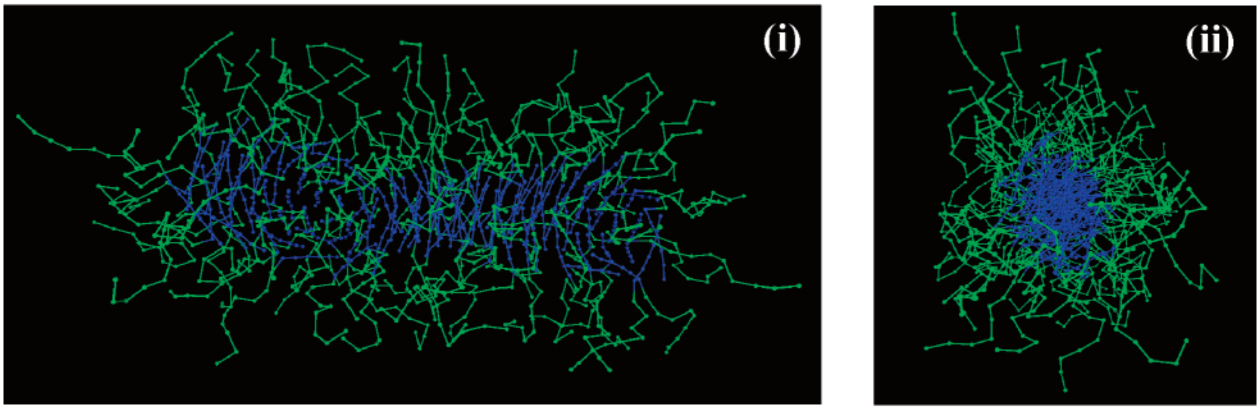

(b) $\varepsilon_{RR} = 2.6$ (i: top view perpendicular to the string axis; ii: side view along the string axis)

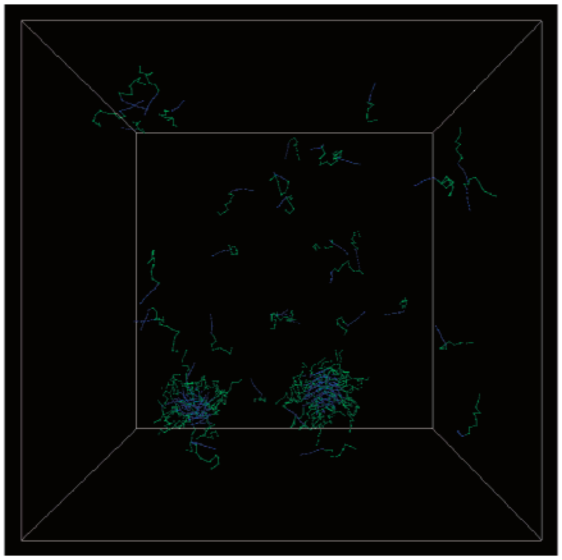

(c) $\varepsilon_{RR} = 2.2$

Figure 3. Snapshot pictures of R_6C_9 copolymer system at different ϵ_{RR}: (a) $\epsilon_{RR} = 3.1$; (b) $\epsilon_{RR} = 2.6$; (c) $\epsilon_{RR} = 2.2$. (a) $\epsilon_{RR} = 3.1$ (i: side view perpendicular to the rod axis; ii: top view along the rod axis), (b) $\epsilon_{RR} = 2.6$ (i: top view perpendicular to the string axis; ii: side view along the string axis), (c) $\epsilon_{RR} = 2.2$.

disk (Figure 5), we may say that the rod blocks form a smectic-like phase in the core of the disk micelle.

The structure of a twisting string is similar to a helix structure with some flexibility in the core of micelle. In order to illustrate such a twisting structure clearly, a typical result of the cosine of twisted angle, $\cos(\psi)$, for the rod alignment is plotted as a function of position along the axis of the string in Figure 7. As can be seen, the absolute value of $\cos(\psi)$ gradually increased

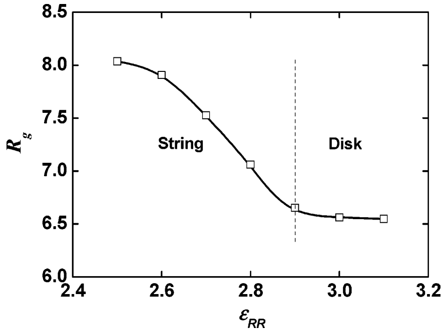

Figure 4. Radius of gyration R_g of micelle for R_6C_9 as a function of ϵ_{RR}.

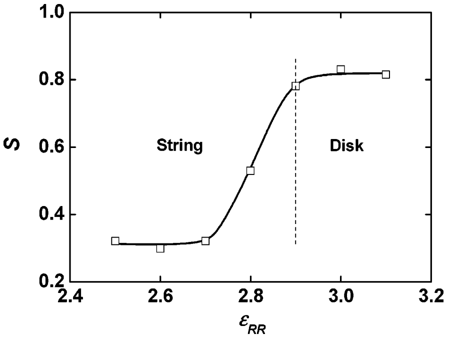

Figure 5. Order parameter *S* of rod blocks in micelle for R_6C_9 as a function of ϵ_{RR}.

to 1.0 and then decreased to 0.0, again and again, along the string axis. Such a periodic change of $\cos(\psi)$ indicates that the rod blocks twistably align to form the core of string micelle, twisting almost linearly (at the constant rate of twisting−angular change) along the axis. Therefore, similar to the helix structure, we can calculate the pitch of twisting (distance between dashed lines shown in Figure 7), which is about 14.8 for this case of $\epsilon_{RR} = 2.6$.

Effects of Coil and Rod Lengths. Figure 8 shows the phase diagrams for rod−coil diblock copolymers, plotted in coil length vs ϵ_{RR} at a fixed rod-bead number $m = 6$. The regions of disk, string, small aggregates, and unimers are constructed. As can be observed in Figure 8, for example (R_6C_9 copolymer), rod−coil copolymers form a disk micelle at high LJ interaction of ϵ_{RR}. A transition from disk to string micelle was found when ϵ_{RR} is decreased, and then the string micelle is broken into small aggregates region. With further decreasing ϵ_{RR}, the system transits into unimers region. On the other hand, no string micelle is observed when the coil length is too short. With increasing the coil block chain length, the regions of small aggregates and string become wider and the onset of the disk formation moves to higher ϵ_{RR}. It suggests that at a constant ϵ_{RR} disk micelle is easy to form for shorter coil length, and the rod−coil blocks tend to form string structure with a long coil. The less effect of coil length on the CMI can also be observed in Figure 8. As the coil length is long enough, the CMI does not change with increasing the coil length.

The effect of rod length on the self-assembly behavior for rod−coil diblock copolymers is also studied. Figure 9 shows the phase diagrams plotted in rod length vs ϵ_{RR} at a fixed coil-bead number $n = 9$. As it can be seen in Figure 9, with increasing the rod block chain length, the regions of small aggregates and string become narrower, and the onset of the disk formation moves to lower ϵ_{RR}. It suggests that at a constant ϵ_{RR} disk micelle is easy to form for longer rod length, and the rod−coil blocks tend to form string structure with a short rod relative to the disk micelle. Such a phase behavior corresponds to that of decreasing the coil length at a constant rod length. Unlike the influence of coil length, a dramatic decrease of CMI with increasing the rod length is found in Figure 9. It confirms the driving forces controlling the self-assembly formation of rod−coil block copolymers are expected to be primarily similar to flexible block copolymers.

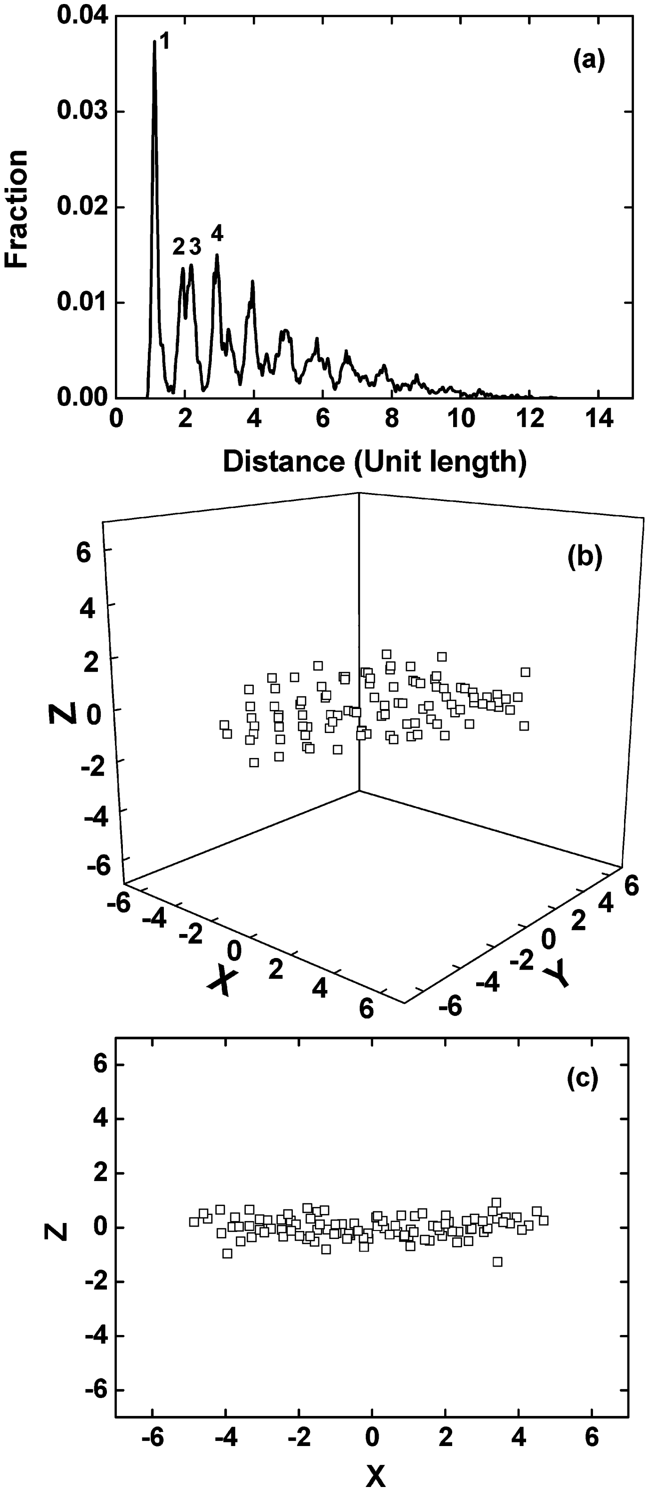

Figure 6. (a) Distance distribution between center positions of rod blocks for R_6C_9 at $\epsilon_{RR} = 3.1$. The first four peak position ratio is about $1{:}\sqrt{3}{:}2{:}\sqrt{7}$. (b) Snapshot of center positions of rod blocks. (c) Plot of *x*- and *z*-component values of center positions of rod blocks.

The influence of chain length on the twisting of rod blocks in the core of string micelle is also examined. The pitches of

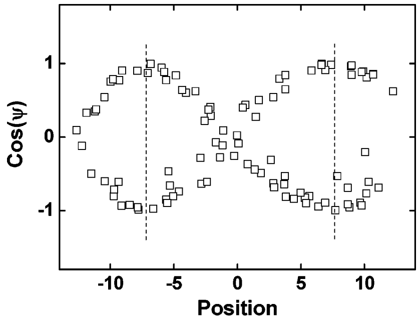

Figure 7. Vector product cos(ψ) for the rod alignment as a function of position along the string axis.

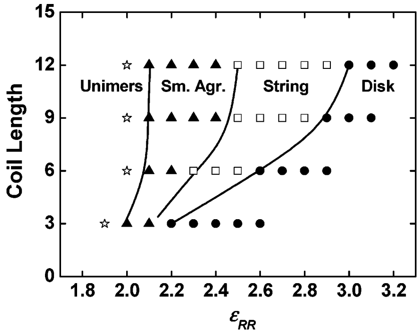

Figure 8. Simulation phase diagrams for rod−coil diblock copolymers plotted in coil length vs ϵ_{RR}. Regions of disk, string, small aggregates, and unimers are shown.

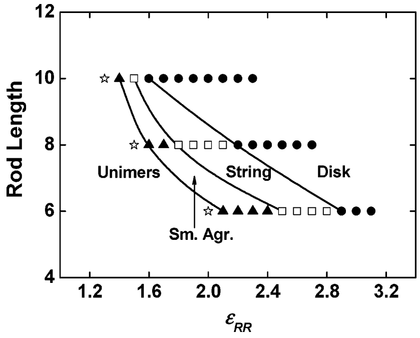

Figure 9. Simulation phase diagrams for rod−coil diblock copolymers plotted in rod length vs ϵ_{RR}. Regions of disk, string, small aggregates, and unimers are shown.

twisting for different lengths of coil blocks and rod blocks are illustrated in parts a and b of Figure 10, respectively. With decreasing the segregation strength ϵ_{RR}, the pitch decreases. It suggests that the alignment of rod blocks is easy to twist at the lower value of ϵ_{RR}. Concomitantly, at a fixed ϵ_{RR}, with increasing the length of coil blocks, a lower value of pitch can be obtained as shown in Figure 10a, which indicates that longer coil chain are easy to form twisting structure in the core of string micelle.

Effects of Temperature. In order to investigate the influence of system temperature on the self-assemble phase behavior, the simulations of three different temperatures (2.8, 3.0, and 3.2) are performed for R_6C_9 copolymers. The simulation phase diagram is plotted in temperature vs ϵ_{RR} in Figure 11. With increasing temperature, the regions of small aggregate and string micelle become wider. The onsets of disk and string formation move to higher segregation strength ϵ_{RR}. It indicates that rod blocks tend to align at the lower temperature, which drives the self-assembled copolymers to form a disk micelle. Concomitantly, an increasing of CMI with increasing system temperature is also found in Figure 11, as expected.

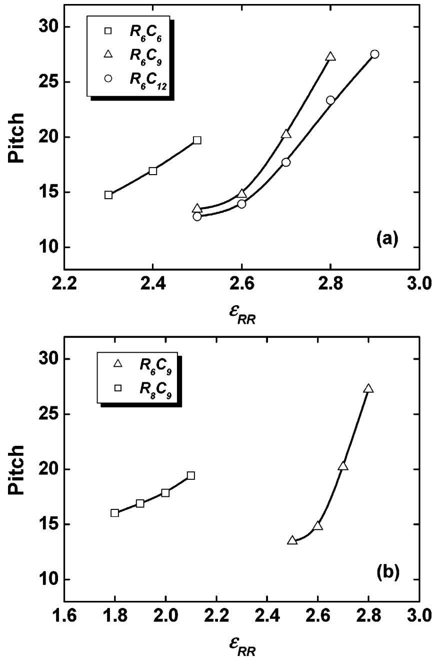

Figure 10. Dependencies of pitch for the twisting of rod blocks in the core of string structure on the rod−coil copolymer chain length: (a) coil length; (b) rod length.

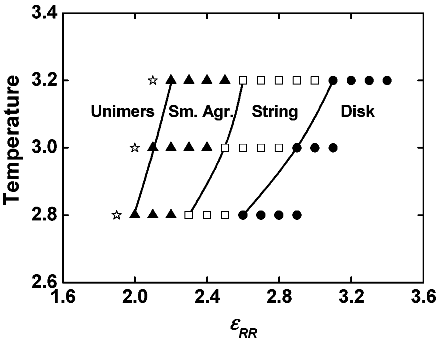

Figure 11. Simulation phase diagrams for rod−coil diblock copolymers plotted in temperature vs ϵ_{RR}. Regions of disk, string, small aggregates, and unimers are shown.

Discussion

Because of the amphiphilic characteristics, rod−coil copolymers can form micelle with rod blocks as the hydrophobic inner core and coil blocks as the hydrophilic corona. On the other hand, the rigidity and asymmetric shape of rod blocks may allow them to assemble with orientational order in the core. In this simulation, it is reasonable for the rod blocks in a coarse-grained model to form a smectic-like order phase as the LJ interaction energy ϵ_{RR} between rod beads is high enough. On the other hand, such a structure induced a higher density of coil blocks in the micelle corona and the rod−coil interface, where the coil chains need more space for movement. As ϵ_{RR} is decreased, the attraction of rod blocks is decreased. Meanwhile, the repulsion of coil blocks becomes dominant to relieve the coil stretching. Here a twisting string is formed due to the combination of enthalpic (or energetic) interaction of rod blocks and conformational entropy of coil blocks. A transition from disk micelle to string micelle occurs with decreasing ϵ_{RR}. As ϵ_{RR} is further decreased, the attractive interaction of rod blocks does not have a large enthalpy enough to form long ordered string, while the coil blocks want more space to explore. As a result, the string micelle is broken into small aggregates. The small aggregates break again, and only dissociative rod−coil copolymers (unimers) exist in the system as the LJ interaction of rod pairs is sufficiently low. Changes of rod length, coil length, and temperature bring about changes of balance between the interaction enthalpy and stretching entropy. The changes of balance may allow us to well understand the effects of chain lengths and temperature on the micelle structure illustrated in Figures 8, 9, and 11.

It is informative to compare the simulation results with experimental observations and theoretical predictions. Lee et al. have reported on rod−coil systems with poly(propylene oxide) (PPO) as coil and a mesogenic rod segment.[8,9] They have investigated phase behavior of rod−coil molecules with different coil lengths and identical rod segments. Rod−coil molecules are found to exhibit monolayered smectic C and smectic A phases at a short coil length. A hexagonal columnar mesophase is formed with increasing the PPO length. Such an observation agrees with our simulation results, as shown in Figure 8. At certain ϵ_{RR}, the rod−coil copolymers form a monolayer disk micelle with a smectic-like phase in the core of micelle, and a transition to string micelle has been found as increasing the coil length. Experimental works have also been performed on systems consisting of molecular rod blocks coupled to polyisoprene.[6,7] The supramolecular structure in the rod−coil systems was observed to vary from lamellar to micellar microphase-separated domains as coil volume fraction is increased. For the theoretical treatment, Williams and Fredrickson suppose a lamellar phase formed by rigid−flexible diblock copolymers previously.[15] They have found hockey puck cylinder structure is stable at large coil fractions. Our simulation result is in agreement with the theoretical prediction of phase transition from layers to cylindrical structure with increasing coil length.

The interesting finding in this paper is that rod−coil diblock copolymers can form the string micelle with the rod blocks twisting in the core under certain condition. Theoretical studies of the possible equilibrium structures of micelles formed by rod−coil block copolymers have been widely reported. But none of them carried out such a twisting string structure. In experiment, it is well-known that chiral molecules can form helical morphologies.[50−52] The helical superstructures obtained from the self-assembly of block copolymers containing chiral blocks are also reported.[53−56] The chiral effects have been demonstrated to be one of the important driving forces to form helical morphologies. The helical superstructure formed by a nonchiral block copolymer was first found by Stadler's group.[57,58] They describe the morphologies of polystyrene-*block*-polybutadiene-*block*-poly(methyl methacrylate) (SBM) triblocks. The helices of B blocks are formed around the cylinder formed by S blocks as reduce the volume fraction of B blocks. In our simulation, a coarse-grained model is used to present the rod−coil copolymer, which can be regard as a common type of rod−coil chain without a specific steric effect. The twisting string formed by such rod−coil copolymers discovered in the simulation can lead to a new method for preparation of helix supermolecules.

It is interesting to investigate the micelle structures in the small aggregation region. Is there spherical micelle existing in this region? In general, the spherical micelle has a definite aggregation number of copolymer chains. In this work, we present many different numbers of rod−coil molecules for simulation, such as 30, 50, 75, 100, 150, and 200. The simulations for different rod lengths (6, 8, and 10) and coil lengths (6, 9, and 12) are also carried out. All of the simulation results show there are different length strings, small disklike, or (and) several copolymers aggregates coexisting with (or without) unimers in the small aggregation region. No micelles of definite aggregation number were found once the string structure is broken. On the other hand, we found the rod block molecules always tend to align to show some order, and they cannot pack radially together to form spherical core of micelle. It suggests there may be no spherical micelle formed by rod−coil copolymers. Such a result agrees with theory prediction by Williams and Fredrickson.[15] They present a theoretical study on cylindrical micelles formed by rigid−flexible diblock copolymers in bulk. It is also argued that spherical micelles probably do not exist because of the difficulty of efficient space-filling packing of rod blocks into a spherical core. For experimental observation, Jenekhe and Chen found poly(phenylquinoline) (PPQ)-*b*-polystyrene rod−coil block copolymers self-assembled into hollow spherical aggregates, where PPQ molecules pack radially in the core.[2] It should be noted that the important contribution to the drive force is strong intermolecular interactions (hydrogen bond) at the rod−coil interface in each block copolymer chain.

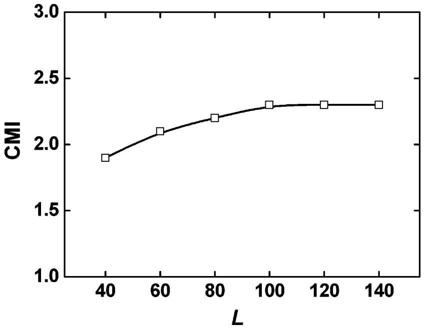

Figure 12. Dependence of critical micelle interaction (CMI) of rod pairs on cell size (*L*).

Before closing the discussion, it is worth pointing out that, in this study, we have not been concerned with the concentration of micellar solution and the aggregation number (and its distribution) of the formed micelles, although they are essential factors in considering stable micelle structures. The problems are rather complicated and difficult in theoretical and computational treatments and are beyond the present study. Still we will present some simulation results on these problems below.

Effects of the copolymer concentration on phase behavior are briefly examined. We define the concentration of rod−coil copolymers as mole concentration $c = n/L^3$, where n is the number of molecules and L is the cell size of simulation. The concentration is varied by changing the cell size, while the number of molecules n is fixed at a value of 100. We perform simulations for systems with a range of cell size L from 40 to 140 (the simulation cell should be large enough to form an isolated string micelle). No new feature has been found for the onset of micelle for string structure and disk structure. But the CMI is slightly changed with increasing cell size L. Figure 12 shows the dependence of CMI on the size of simulation cell. It is clearly seen that the critical micelle interaction CMI is first increased and tends to level off with increasing cell size L.

The simulations for aggregation number n_{agg} of rod−coil copolymers with a range from 30 to 200 are performed at a fixed value of cell size $L = 60$. It should be noted that the change of n_{agg} also brings about change in the concentration of rod−coil copolymers. A slight increase of CMI has been found as n_{agg} is increased. No string micelle is found when the simulations performed for too small n_{agg} (such as 30). For the larger n_{agg}, the onsets of string and disk micelle do not change with n_{agg}, and a more flexible string is found.

Conclusion

Brownian dynamics is first used to simulate the self-assembly behavior of rod–coil diblock copolymers. The micelle structure and molecular packing of rod blocks are discussed. Aggregate structure transitions are found as change segregation strength of rod pairs. Diagrams for the regions of thermodynamic stability of disk, string, and small aggregates are constructed. The influences of chain length and temperature on the self-assembly behavior are also presented. Some simulation results are in agreement with the existing experimental observations and theoretical predictions. The main results can be summarized as follows:

(1) An available new coarse-grained model for rod–coil diblock copolymer is presented. The molecule is realized by a linear chain consisting of definite beads connecting by harmonic bond stretching potential. The rigidity of rod block is introduced by harmonic angle bend potential. The self-assembly behavior of such copolymers are successfully performed by the Brownian dynamics simulation approach.

(2) The micelle structures of disk and string can be formed by rod–coil diblock copolymer. The structure transitions from disk to string and further to some broken small aggregates are presented by changing segregation strength of rod pairs. For the disk micelle, the rod blocks tend to align orientationally to form a smectic-like phase in the core. A new string micelle is found, where the rod blocks twistably pack in the core like a helical structure, with decreasing rod pair interaction.

(3) The influences of chain length and temperature on the self-assembly phase diagrams are carried out. It was found the onsets of micelle formations of disk and string moved to higher LJ rod pair interaction with decreasing rod block length or (and) increasing the coil length or (and) temperature. Meanwhile, the regions of string micelle and small aggregate became widened.

(4) Some simulation results agree with existing experiments and theoretical predictions. It is argued that the spherical micelle may be not formed by rod–coil diblock in such a model.

Acknowledgment. This work was supported by a Grant-in-Aid for "Academic Frontier" Project for Private Universities; matching fund subsidy from Ministry of Education, Culture, Sports, Science and Technology (MEXT), 2001–2005 and 2006–2008, and by National Natural Science Foundation of China (20574018, 50673026). Support from Program for New Century Excellent Talents in University in China (NCET-04-0410) is also appreciated.

References and Notes

(1) Jenekhe, S. A.; Chen, X. L. *Science* **1998**, *279*, 1903–1906.
(2) Jenekhe, S. A.; Chen, X. L. *Science* **1999**, *283*, 372–375.
(3) Chen, J. T.; Thomas, E. L.; Ober, C. K.; Mao, G.-P. *Science* **1994**, *273*, 343–346.
(4) Chen, J. T.; Thomas, E. L.; Ober, C. K.; Hwang, S. S. *Macromolecules* **1995**, *28*, 1688–1697.
(5) Chochos, C. L.; Tsolakis, P. K.; Gregoriou, V. G.; Kallitsis, J. K. *Macromolecules* **2004**, *37*, 2502–2510.
(6) Radzilowski, L. H.; Stupp, S. I. *Macromolcecules* **1994**, *27*, 7747–7753.
(7) Stupp, S. I.; LeBonheur, V.; Walker, K.; Li, L. S.; Huggins, K. E.; Keser, M.; Amstutz, A. *Science* **1997**, *276*, 384–389.
(8) Lee, M.; Cho, B. K.; Zin, W. C. *Chem. Rev.* **2001**, *101*, 3859–3892.
(9) Lee, M.; Cho, B. K.; Kim, H.; Yoon, J. Y.; Zin, W. C. *J. Am. Chem. Soc.* **1998**, *120*, 9168–9179.
(10) Park, J. W.; Thomas, E. L. *Macromolecules* **2004**, *37*, 3532–3535.
(11) Wu, J.; Pearce, E. M.; Kwei, T. K.; Lefebvre, A. A.; Balsara, N. P. *Macromolecules* **2002**, *35*, 1791–1796.
(12) Halperin, A. *Macromolecules* **1990**, *23*, 2724–2731.
(13) Semenov, A. N.; Vasilenco, S. V. *Sov. Phys. JETP* **1986**, *63*, 70–79.
(14) Semenov, A. N. *Mol. Cryst. Liq. Cryst.* **1991**, *209*, 191–196.
(15) Williams, D. R. M.; Fredrickson, G. H. *Macromolecules* **1992**, *25*, 3561–3568.
(16) Muller, M.; Schick, M. *Macromolecules* **1996**, *29*, 8900–8903.
(17) Raphael, E.; de Gennes, P. G. *Makromol. Chem., Macromol. Symp.* **1992**, *62*, 1–16.
(18) Matsen, M. W.; Barrett, C. *J. Chem. Phys.* **1998**, *109*, 4108–4118.
(19) Li, W. T.; Gersappe, D. *Macromolecules* **2001**, *34*, 6783–6789.
(20) Kim, S. H.; Jo, W. H. *Macromolecules* **2001**, *34*, 7210–7218.
(21) Larson, R. G. *Macromolecules* **1994**, *27*, 4198–4203.
(22) Viduna, D.; Milchev, A.; Binder, K. *Macromol. Theory Simul.* **1998**, *7*, 649–658.
(23) Milchev, A.; Bhattacharya, A.; Binder, K. *Macromolecules* **2001**, *34*, 1881–1893.
(24) Hoffmann, A.; Sommer, J. U.; Blumen, A. *J. Chem. Phys.* **1999**, *107*, 7559–7570.
(25) Yu, B.; Li, B. H.; Sun, P. C.; Chen, T. H.; Jin, Q. H.; Ding, D. T.; Shi, A. C. *J. Chem. Phys.* **2005**, *123*, 234902-1–8.
(26) Murat, M.; Grest, G. S.; Kremer, K. *Macromolecules* **1999**, *32*, 595–609.
(27) Schultz, A. J.; Hall, G. K.; Genzer, J. *J. Chem. Phys.* **2002**, *117*, 10329–10338.
(28) Schultz, A. J.; Hall, G. K.; Genzer, J. *Macromolecules* **2005**, *38*, 3007–3016.
(29) Alsunaidi, A.; Abu-Sharkh, B. F. A. *J. Chem. Phys.* **2003**, *119*, 9894–9902.
(30) Chushak, Y.; Travesset, A. *J. Chem. Phys.* **2005**, *123*, 234905-1–7.
(31) Tsige, M.; Mattsson, T. R.; Grest, G. S. *Macromolecules* **2004**, *37*, 9132–9138.
(32) Groot, R. D.; Madden, T. J. *J. Chem. Phys.* **1998**, *108*, 8713–8724. Groot, R. D.; Madden, T. J.; Tildesley, D. J. *J. Chem. Phys.* **1999**, *108*, 9737–9749.
(33) Qian, H. J.; Lu, Z. Y.; Chen, L. J.; Li, Z. S.; Sun, C. C. *Macromolecules* **2005**, *38*, 1395–1401.
(34) Guo, H. X.; de la Gruz, M. O. *J. Chem. Phys.* **2005**, *123*, 174903-1–10.
(35) AlSunaidi, A.; den Otter, W. K.; Clarke, J. H. R. Phil. *Trans. R. Soc. London A* **2004**, *362*, 1773–1781.
(36) Affouard, F.; Kroger, M.; Hess, S. *Phys. Rev. E* **1996**, *54*, 5178–5186.
(37) Van Duijneveldt, J.; Gil-Vellegas, A.; Jackson, G.; Allen, M. P. *J. Chem. Phys.* **2000**, *112*, 9092–9104.
(38) Nichlas, K.; Bopp, P.; Brickmann, J. *J. Chem. Phys.* **1994**, *101*, 3157–3171.
(39) McBride, C.; Vega, C.; MacDowell, L. G. *Phys. Rev. E* **2001**, *64*, 011703-1–14.
(40) von Gottberg, F. K.; Smith, K. A.; Hatton, T. A. *J. Chem. Phys.* **1997**, *106*, 9850–9857.
(41) http://octa.jp.
(42) Lin, S.; Numasawa, N.; Nose, T.; Lin, J. *Polym. Prepr., Jpn.* **2005**, *54*, 1066.
(43) Bourov, G. K.; Bhattacharya, A. *J. Chem. Phys.* **2003**, *119*, 9219–9225.
(44) Bourov, G. K.; Bhattacharya, A. *J. Chem. Phys.* **2005**, *122*, 044702-1–6.
(45) Maier, M.; Saupe, A. *Naturforsch. Z.* **1959**, *14A*, 882–889; *Naturforsch. Z.* **1960**, *15A*, 287–292.
(46) de Gennes, P. G. *The Physics of Liquid Crystals*; Clarendon Press: Oxford, 1974.
(47) Chandrasekhar, S. *Liquid Crystal*; Cambridge University Press: London, 1977.
(48) Grest, G. S.; Kremer, K. *Phys. Rev. A* **1986**, *33*, 3628–3631.
(49) Grest, G. S.; Lacasse, M. D. *J. Chem. Phys.* **1996**, *105*, 10583–10594.
(50) Li, C. Y.; Cheng, S. Z. D.; Ge, J. J.; Bai, F.; Zhang, J. Z.; Mann, I. K.; Harris, F. W.; Chien, L. C.; Yan, D.; He, T.; Lotz, B. *Phys. Rev. Lett.* **1999**, *83*, 4558–4561.
(51) Vriezema, D. M.; Hoogboom, J.; Velonia, K.; Takazawa, K.; Christianen, P. C. M.; Maan, J. C.; Rowan, A. E.; Nolte, R. J. M. *Angew. Chem., Int. Ed.* **2003**, *42*, 772–776.
(52) Li, B. S.; Cheuk, K. K. L.; Salhi, F.; Lam, J. W. Y.; Cha, J. A. K.; Xiao, X.; Bai, C.; Tang, B. Z. *Nano. Lett.* **2001**, *1*, 323–328.
(53) Cornelissen, J. J. L. M.; Fischer, M.; Sommerdijk, N. A. J. M.; Nolte, R. J. M. *Science* **1998**, *280*, 1427–1430.
(54) Rowan, A. E.; Nolte, R. J. M. *Angew. Chem., Int. Ed.* **1998**, *37*, 63–68.
(55) Ho, R. M.; Chiang, Y. W.; Tsai, C. C.; Lin, C. C.; Ko, B. T.; Huang, B. H. *J. Am. Chem. Soc.* **2004**, *126*, 2704–2705.
(56) Sung, C. H.; Kung, L. R.; Hsu, C. S.; Lin, T. F.; Ho, R. M. *Chem. Mater.* **2006**, *18*, 352–359.
(57) Stadler, R.; Auschra, C.; Bechmann, J.; Krappe, U.; Voigt-Martin, I.; Leibler, L. *Macromolecules* **1995**, *28*, 3080–3097.
(58) Breiner, U.; Krappe, U.; Abetz, V.; Stadler, R. *Macromol. Chem. Phys.* **1997**, *198*, 1051–1083.

MA062064L